


The complex viscosity of Möbius macromolecules

Cite as: Phys. Fluids **32**, 093107 (2020); <https://doi.org/10.1063/5.0022546>

Submitted: 21 July 2020 . Accepted: 11 August 2020 . Published Online: 28 September 2020

Jourdain H. Piette , Nicolas Moreno , Eliot Fried , and Alan Jeffrey Giacomin 

COLLECTIONS

 This paper was selected as Featured



View Online



Export Citation



CrossMark

ARTICLES YOU MAY BE INTERESTED IN

[Weather impact on airborne coronavirus survival](#)

Physics of Fluids **32**, 093312 (2020); <https://doi.org/10.1063/5.0024272>

[Anchoring mechanisms of a holder-stabilized premixed flame in a preheated mesoscale combustor](#)

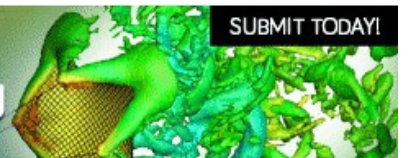
Physics of Fluids **32**, 097103 (2020); <https://doi.org/10.1063/5.0021864>

[Effect of thermal convection on thermocapillary migration of a surfactant-laden droplet in a microchannel](#)

Physics of Fluids **32**, 092009 (2020); <https://doi.org/10.1063/5.0021312>

Physics of Fluids
Special Issue on the **Lattice Boltzmann Method**

SUBMIT TODAY!



The complex viscosity of Möbius macromolecules

Cite as: *Phys. Fluids* **32**, 093107 (2020); doi: [10.1063/5.0022546](https://doi.org/10.1063/5.0022546)

Submitted: 21 July 2020 • Accepted: 11 August 2020 •

Published Online: 28 September 2020



View Online



Export Citation



CrossMark

Jourdain H. Piette,¹  Nicolas Moreno,^{2,3}  Eliot Fried,²  and Alan Jeffrey Giacomin^{1,4,5,6} 

AFFILIATIONS

¹Chemical Engineering Department, Queen's University, Kingston, Ontario K7L 3N6, Canada

²Mathematics, Mechanics, and Materials Unit, Okinawa Institute of Science and Technology, Okinawa, Japan

³CFD Modelling and Simulation Group, Basque Center for Applied Mathematics, University of the Basque Country, Bilbao 48009, Spain

⁴Mechanical and Materials Engineering Department, Queen's University, Kingston, Ontario K7L 3N6, Canada

⁵Physics, Engineering Physics and Astronomy Department, Queen's University, Kingston, Ontario K7L 3N6, Canada

⁶Mechanical Engineering Department, University of Nevada, Reno, Nevada 89557, USA

^{a)} Author to whom correspondence should be addressed: giacomin@queensu.ca

ABSTRACT

Using general rigid bead–rod theory, we explore the effect of twisting a macromolecule on its rheological properties in suspensions. We thus focus on macromolecules having the form of Möbius bands so that the number of twists can be incremented. We call these *Möbius macromolecules*. When represented in general rigid bead–rod theory, these macromolecules comprise beads whose centers all fall on a Möbius band. From first principles, we calculate the complex viscosity of twisted rings with zero to seven twists. We find that the zero-shear values of the viscosity and first normal stress coefficient increase with twisting. Furthermore, we find that the real part of the complex viscosity descends more rapidly, with frequency, with extent of twist. For the imaginary part of the complex viscosity, the more twisted, the higher the peak. For each part of the dimensionless complex viscosity and the first normal stress coefficient, the results fall on one of just three curves corresponding to zero, even, or odd numbers of twists. We also explore the effects of the length and the aspect ratio of twisted macromolecular suspensions. We close with a worked example for a suspension of triply twisted Möbius annulene.

© 2020 Author(s). All article content, except where otherwise noted, is licensed under a Creative Commons Attribution (CC BY) license (<http://creativecommons.org/licenses/by/4.0/>). <https://doi.org/10.1063/5.0022546>

I. INTRODUCTION

General rigid bead–rod theory affords the opportunity to explore how the macromolecular shape, even if complex, affects the rheology of polymeric liquids. We explore how twisting a macromolecule affects its complex viscosity. Previously, we studied the effect of twisting on linear chains, such as doubly helical macromolecules, including deoxyribonucleic acid (see Subsection V C of Ref. 1). However, for linear helical macromolecules, the chain length is proportional to the number of twists, so the effect of twisting is confounded by the chain length. We therefore explore the role of the number of twists in ring polymers on complex viscosity. Adding one or more twists to ring polymers produces Möbius macromolecules, which we define mathematically below. Although this work is mainly driven by curiosity,² its applications have not

escaped our attention. For instance, to introduce chemical stability, organic chemists twist pi-bonded structures into ringed macromolecules.³ The more twisted, the more stable the macromolecule might be.^{2,3} For our symbols, dimensional and non-dimensional, listed in Tables I and II, we follow those of the corresponding textbook treatments, Example 16.7-1 of Ref. 4 or Example 13.6-1 of Ref. 5.

For linear viscoelastic behaviors, general rigid bead–rod theory has been evaluated for only a few very simple structures: rigid rings, the rigid tridumbbell, and three quadra-functional branched structures along a backbone (Table 16.7-1 of Ref. 5). More ambitiously, and still unpublished, recent work attacks other branch functionalities along a backbone, star branched architectures, be they planar or polyhedral,⁶ and diblock copolymers.⁷ For oscillatory shear flow, the frequency dependencies of both parts of the complex viscosity are

TABLE I. Dimensional variables. Legend: $M \equiv$ mass, $L \equiv$ length, $t \equiv$ time, and $T \equiv$ temperature.

Name	Symbol	Dimensions
Absolute temperature	T	T
Angular frequency	ω	t^{-1}
Band width	w	L
Boltzmann constant	k_B	ML^2/Tt^2
Cartesian coordinates	x,y,z	L
Cylindrical angular coordinate	θ	rads
Equilibrium center to center separation	L	L
Extra stress tensor	τ	M/Lt^2
Friction constant	ζ	M/t
Lateral position across the strip	s	L
Normal stress coefficient, first, displacement	Ψ_1^d	M/L
Normal stress coefficient, first, minus imaginary part	Ψ_1''	M/L
Normal stress coefficient, first, real part	Ψ_1'	M/L
Normal stress coefficient, first, complex	$\Psi_1^* = \Psi_1' - i\Psi_1''$	M/L
Normal stress coefficient, first, zero-shear	$\Psi_{1,0}$	M/L
Number of twists, integer	τ	Twists
Radius, circle of support	R	L
Relaxation time	λ	t
Shear rate	$\dot{\gamma}$	t^{-1}
Shear rate amplitude	$\dot{\gamma}^0$	t^{-1}
Time	t	t
Trigonometric shift [Eq. (35)]	κ	rads
Viscosity, complex	$\eta^* \equiv \eta' - i\eta''$	M/Lt
Viscosity, complex, minus imaginary part	η''	M/Lt
Viscosity, complex, real part	η'	M/Lt
Viscosity, solvent	η_s	M/Lt
Viscosity, zero-shear	η_0	M/Lt

predicted qualitatively. By *qualitatively*, we mean that the real part of the complex viscosity descends with frequency from its asymptotic zero-shear value and then inflects with frequency, while the imaginary part rises and then falls.⁸

TABLE III. Möbius bands with three rows and an aspect ratio of twenty.

Twists	I_1	I_3	a	b	v	$2b/av$	λ/λ_0	$\frac{\eta_0 - \eta_s}{nk_B T \lambda}$	$\frac{\Psi_{1,0}}{nk_B T \lambda^2}$
0	1548.774	2995.258	745.28	0.5234	0.003 874	0.3625	3097.549	1.9670	1.0643
1	1537.670	3023.265	729.38	0.5600	0.003 902	0.3936	3075.340	1.9831	1.1297
2	1125.685	2205.196	535.72	0.5518	0.005 330	0.3865	2251.371	1.9795	1.1150
3	1420.718	2794.051	673.74	0.5606	0.004 223	0.3941	2841.437	1.9833	1.1307
4	1882.388	3702.388	892.59	0.5609	0.003 187	0.3943	3764.776	1.9834	1.1311
5	1365.395	2685.078	647.54	0.5605	0.004 394	0.3940	2730.790	1.9833	1.1305
6	984.935	1937.258	467.03	0.5609	0.006 092	0.3943	1969.870	1.9834	1.1312

TABLE II. Dimensionless variables and groups.

Name	Symbol
Aspect ratio	R/w
Orientation constant [Eq. (22)]	a
Orientation constant [Eq. (23)]	b
Orientation constant [Eq. (24)]	v
Bead row index	j
Bead rows, number of	J
Bead position index	k
Beads in each row	K
Deborah number, oscillatory shear	$De \equiv \lambda\omega$
Weissenberg number	$Wi \equiv \lambda\dot{\gamma}^0$

From general rigid bead-rod theory, the viscous contribution to the dimensionless complex viscosity is given by [Eq. (40) of Ref. 9]

$$\frac{\eta' - \eta_s}{\eta_0 - \eta_s} = \left(\frac{1}{2b/av} + 1 \right)^{-1} \left(\frac{1}{2b/av} + \frac{1}{1 + (\lambda\omega)^2} \right) \quad (1)$$

and *minus* the elastic contribution by [Eq. (41) of Ref. 9]

$$\frac{\eta''}{\eta_0 - \eta_s} = \left(\frac{1}{2b/av} + 1 \right)^{-1} \frac{\lambda\omega}{1 + (\lambda\omega)^2}, \quad (2)$$

which are subject to the definition of small-amplitude oscillatory shear flow (SAOS) [Eq. (31) of Ref. 9],

$$\lambda\dot{\gamma}^0 \ll \frac{1}{v\sqrt{2}}, \quad (3)$$

which is a restriction we will also use below.

By substituting Eqs. (64)–(66) of Ref. 9 into Eqs. (68)–(70) of Ref. 9, Kanso and Giacomin bridged continuum theory to macromolecular, yielding expressions for the normal stress difference responses from general rigid bead-rod theory. By continuum theory, we mean any case of the Oldroyd 8-constant framework (see Table III of Ref. 10 and Table I of Refs. 11 and 12), including the corotational Jeffreys model. The coefficients of the displacement term of

TABLE IV. Möbius bands with three rows and an aspect ratio of ten.

Twists	I_1	I_3	a	b	ν	$2b/av$	λ/λ_0	$\frac{\eta_0 - \eta_s}{nk_B T \lambda}$	$\frac{\Psi_{1,0}}{nk_B T \lambda^2}$
0	214.6036	377.6226	109.7048	0.3462	0.02796	0.2258	429.2071	1.8798	0.7367
1	209.1659	391.5534	103.1734	0.4562	0.02869	0.3083	418.3318	1.9360	0.9426
2	115.2762	213.3275	57.3000	0.4341	0.05205	0.2911	230.5524	1.9253	0.9019
3	157.3290	295.1023	77.4970	0.4601	0.03814	0.3114	314.6580	1.9379	0.9497
4	226.2647	424.7007	111.3990	0.4615	0.02652	0.3124	452.5293	1.9385	0.9523
5	139.9470	262.4252	68.9486	0.4596	0.04287	0.3109	279.8941	1.9376	0.9487
6	84.3479	158.3068	41.5305	0.4613	0.07113	0.3123	168.6957	1.9384	0.9519

TABLE V. Möbius bands with seven rows and an aspect ratio of ten.

Twists	I_1	I_3	a	b	$\nu \times 10^{-3}$	$2b/av$	λ/λ_0	$\frac{\eta_0 - \eta_s}{nk_B T \lambda}$	$\frac{\Psi_{1,0}}{nk_B T \lambda^2}$
0	12 847.5031	23 550.3026	6424.3269	0.4164	0.4670	0.2776	25 695.0062	1.9165	0.8691
1	12 383.3944	23 699.3317	6009.5876	0.5010	0.4845	0.3441	24 766.7888	1.9569	1.0241
2	6 889.4652	13 057.4891	3368.3107	0.4809	0.8709	0.3279	13 778.9303	1.9476	0.9877
3	9 952.2323	19 055.0158	4828.0793	0.5019	0.6029	0.3449	19 904.4646	1.9573	1.0258
4	14 249.9226	27 289.1107	6911.8948	0.5024	0.4211	0.3452	28 499.8452	1.9575	1.0266
5	7 873.3171	15 072.8281	3819.9030	0.5017	0.7621	0.3447	15 746.6341	1.9572	1.0253
6	4 738.0159	4 738.0159	2298.0951	0.5024	1.2664	0.3453	9 476.0315	1.9576	1.0267

TABLE VI. Möbius bands with seven rows and an aspect ratio of seven.

Twists	I_1	I_3	a	b	$\nu \times 10^{-3}$	$2b/av$	λ/λ_0	$\frac{\eta_0 - \eta_s}{nk_B T \lambda}$	$\frac{\Psi_{1,0}}{nk_B T \lambda^2}$
0	4904.7733	8293.7032	2548.8953	0.2864	1.2233	0.1837	429.2071	1.8455	0.6209
1	4569.7701	8393.6137	2282.2573	0.4201	1.3130	0.2804	418.3318	1.9184	0.8760
2	2074.6151	3744.4869	1046.8013	0.3887	2.8921	0.2568	230.5524	1.9025	0.8173
3	3078.3776	5660.9635	1536.2909	0.4223	1.9491	0.2821	314.6580	1.9195	0.8800
4	4109.8159	7562.1381	2050.2919	0.4234	1.4599	0.2829	452.5293	1.9200	0.8820
5	2144.6821	3942.7513	1070.5244	0.4217	2.7976	0.2816	279.8941	1.9191	0.8790
6	1203.3400	2214.3663	600.2849	0.4235	4.986	0.2830	168.6957	1.9201	0.8823

TABLE VII. Zero-shear viscosities and first normal stress coefficients made dimensionless with λ_0 .

Twists	Table III		Table IV		Table V		Table VI		Table VIII	
	$\frac{\eta_0 - \eta_s}{nk_B T \lambda_0}$	$\frac{\Psi_{1,0}}{nk_B T \lambda_0^2}$	$\frac{\eta_0 - \eta_s}{nk_B T \lambda_0}$	$\frac{\Psi_{1,0}}{nk_B T \lambda_0^2}$	$\frac{\eta_0 - \eta_s}{nk_B T \lambda_0}$	$\frac{\Psi_{1,0}}{nk_B T \lambda_0^2}$	$\frac{\eta_0 - \eta_s}{nk_B T \lambda_0}$	$\frac{\Psi_{1,0}}{nk_B T \lambda_0^2}$	$\frac{\eta_0 - \eta_s}{nk_B T \lambda_0}$	$\frac{\Psi_{1,0}}{nk_B T \lambda_0^2}$
0	6092.8789	3508.7006	806.8235	232.9423	49 244.4794	19 408.3326	792.1017	165.4666
1	6098.7068	3924.8169	809.8904	371.6857	48 466.1290	25 974.9328	802.5277	321.0178
2	4458.5684	2798.9608	443.8825	187.5368	26 835.8447	13 442.0533	438.6259	154.0042
3	5635.422	3632.7274	609.7757	283.7995	38 959.0086	20 944.7842	603.9860	243.6711	2463.1281	154.6226
4	1882.388	5582.6812	877.2280	410.3877	55 788.4470	30 036.2023	868.8563	352.0334
5	5415.9758	3490.0322	542.3228	251.9135	30 819.3123	16 553.4930	537.1448	216.2577
6	3907.0402	2520.6721	326.9997	152.8574	18 550.2793	9 988.8069	323.9126	131.3217

the normal stress differences in SAOS are [Eq. (71) of Ref. 9 and Refs. 11 and 13]

$$\frac{\Psi_1^d}{nkT\lambda^2} = \frac{b}{1 + (\lambda\omega)^2} \tag{4}$$

and of the parts that are in-phase with $\cos 2\omega t$ [Eq. (72) of Ref. 9],

$$\frac{\Psi_1'}{nkT\lambda^2} = b \frac{(1 - 2(\lambda\omega)^2)}{(1 + (\lambda\omega)^2)(1 + 4(\lambda\omega)^2)} \tag{5}$$

and out-of-phase with $\cos 2\omega t$ [Eq. (73) of Ref. 9],

$$\frac{\Psi_1''}{nkT\lambda^2} = 3b \frac{\lambda\omega}{(1 + (\lambda\omega)^2)(1 + 4(\lambda\omega)^2)}, \tag{6}$$

which goes through a maximum, as does $\eta''/(\eta_0 - \eta_s)$ of Eq. (2).^{9,13} Below, we will capitalize on Eqs. (4)–(6) subject to Eq. (3) to study the effect of architecture on Möbius macromolecules.

Since general rigid bead–rod theory relies entirely on macromolecular orientation for explaining rheological responses of macromolecular suspensions,¹⁷ the theory neglects interactions between macromolecules. We are attracted to general rigid bead–rod theory for the accuracy of its predictions for its simplest special cases and to the rigid dumbbell, at least qualitatively, for most of the viscoelastic material functions measured in the laboratory (see Introduction of Refs. 9, 10, 15, and 16). Perhaps the reason for the apparent success of the rigid dumbbell, even for flexible macromolecules, is that the overall orientation of the molecule is the most important factor in determining the rheological responses of elastic liquids. The chain expansion and contraction seem to be less important. Furthermore, the successes (Fig. 20 of Ref. 1, Fig. 14 of Ref. 9, and Fig. 2 of Ref. 16) of general rigid bead–rod theory for concentrated systems suggests that interactions between macromolecules are also less important.

II. METHOD

We study macromolecules whose bead positions all lie on the surfaces of Möbius bands, with τ twists, given by

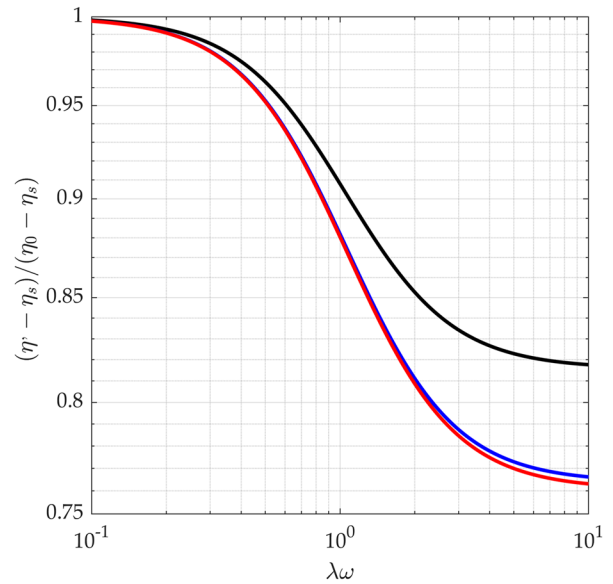
$$\begin{bmatrix} x \\ y \\ z \end{bmatrix} = \begin{bmatrix} \{R + s\sin\frac{1}{2}\tau\theta\}\cos\theta \\ \{R + s\sin\frac{1}{2}\tau\theta\}\sin\theta \\ s\cos\frac{1}{2}\tau\theta \end{bmatrix}, 0 \leq \theta \leq 2\pi, \tag{7}$$

$$-\frac{1}{2}w \leq s \leq \frac{1}{2}w, \tau = 0, 1, 2, \dots,$$

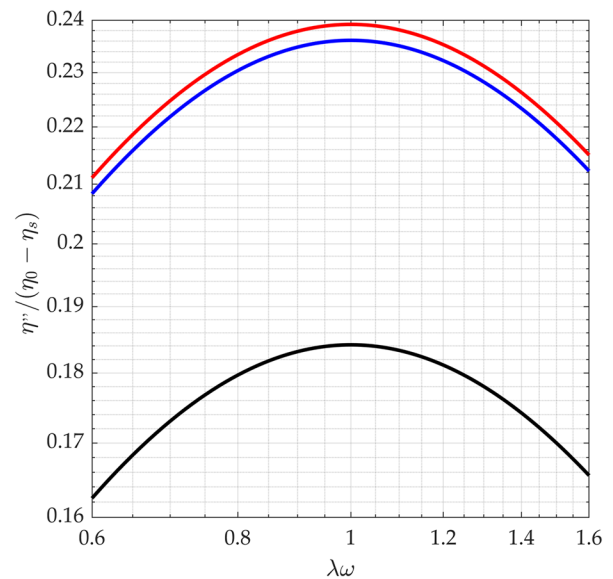
where w is the strip width, s is the lateral position across the strip, θ is the cylindrical angular coordinate, and τ is the integer number of twists. The cylindrical angular coordinate, θ , thus defines the position along the strip. We call macromolecules whose bead positions satisfy Eq. (7) *Möbius macromolecules*. Otherwise put, Möbius macromolecules are objects whose representations in general rigid bead–rod theory comprise beads whose centers fall on Möbius bands. Equation (7) is parametric in θ , and all bands described by it intersect at the *circle of support* of radius R ,

$$\begin{bmatrix} x \\ y \\ z \end{bmatrix} = \begin{bmatrix} R\cos\theta \\ R\sin\theta \\ 0 \end{bmatrix}, 0 \leq \theta \leq 2\pi. \tag{8}$$

Without twists, $\tau = 0$, and Eq. (7) reduces to the parametric equation for a right circular cylinder,



(a)



(b)

FIG. 1. [(a) and (b)] Effect number of twists on the viscoelastic response [Eqs. (1) and (2)]. No twists (**black**), even number of twists (**red**) (Fig. 10), and odd number of twists (**blue**) (Fig. 11). Möbius bands from three rows of beads with aspect ratio ten.

$$\begin{bmatrix} x \\ y \\ z \end{bmatrix} = \begin{bmatrix} R\cos\theta \\ R\sin\theta \\ s \end{bmatrix}, 0 \leq \theta \leq 2\pi, -\frac{1}{2}w \leq s \leq \frac{1}{2}w. \quad (9)$$

Thus, we will compare twisted structures, exploring one to seven twists, with their untwisted counterpart, this right circular cylinder.

When modeling Möbius macromolecules using general rigid bead-rod theory, we begin with a set of rigidly spaced beads with position vector \mathbf{r}_i , where the macromolecular center of mass \mathbf{R} satisfies

$$\sum_{i=1}^N m_i(\mathbf{r}_i - \mathbf{R}) = 0 \quad (10)$$

so that

$$\mathbf{R} = \frac{1}{M} \sum_{i=1}^N m_i \mathbf{r}_i, \quad (11)$$

where the subscript i indicates the bead number, N is the total number of beads, and $M \equiv \sum_{i=1}^N m_i$ is the molecular weight. Since we

construct our Möbius macromolecules with identical beads of diameter d and mass m , the molecular weight is given by $M \equiv mN$, and thus, the center of mass is

$$\mathbf{R} = \frac{1}{N} \sum_{i=1}^N \mathbf{r}_i, \quad (12)$$

which we will use below.

We next install molecular coordinates at the macromolecular center of mass, and we orient these Cartesian coordinates such that $\hat{\delta}_3$ is along the polar axis of the moment of inertia ellipsoid (MIE). The position vector of the i th bead with respect to the center of mass is given by [Eq. (16.7-16) of Ref. 4 or Eq. (13.6-16) of Ref. 6]

$$\mathbf{R}_i \equiv [r_{i1}, r_{i2}, r_{i3}] - \mathbf{R}. \quad (13)$$

Equation (7) refers to a coordinate system whose origin is arbitrarily set at the position $[0,0,0]$. To get \mathbf{R}_i , we insert Eq. (7) into Eq. (12) to get \mathbf{R} and then this into Eq. (13).

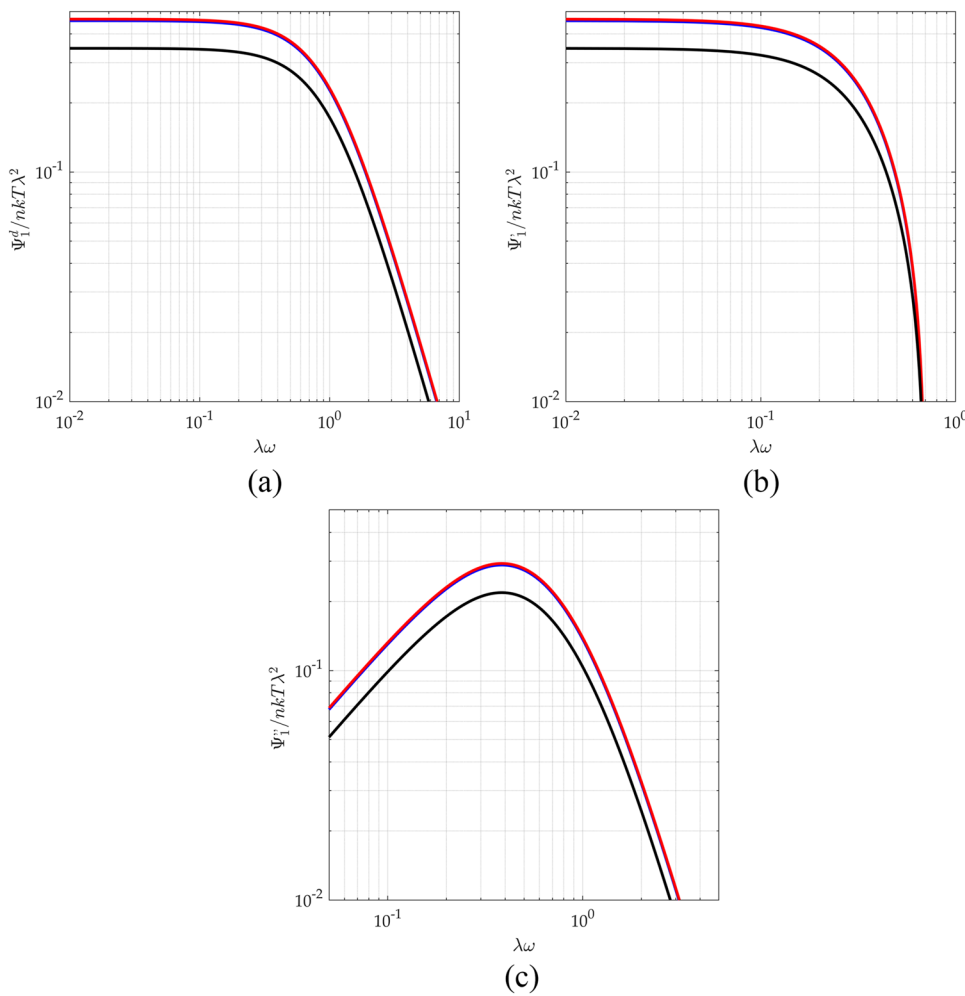


FIG. 2. [(a)–(c)] Effect number of twists on the first normal stress difference [Eqs. (4), (5), and (6)]. No twists (**black**), even number of twists (**red**) (Fig. 10), and odd number of twists (**blue**) (Fig. 11). Möbius bands from three rows of beads with aspect ratio ten.

Thus, combining Eq. (7) with (13) gives for our Möbius macromolecules

$$\begin{bmatrix} R_{i,1} \\ R_{i,2} \\ R_{i,3} \end{bmatrix} = \begin{bmatrix} \{R + s_k \cos \frac{1}{2} \tau \theta_j\} \cos \theta_j \\ \{R + s_k \cos \frac{1}{2} \tau \theta_j\} \sin \theta_j \\ s_k \sin \frac{1}{2} \tau \theta_j \end{bmatrix}, 0 \leq \theta_j \leq 2\pi, \quad (14)$$

$$-\frac{1}{2}w \leq s_k \leq \frac{1}{2}w, \tau = 0, 1, 2, \dots,$$

where the bead rows across the Möbius strip are numbered $j = 1, 2, \dots, J$ and the bead positions along the rows, $k = 1, 2, \dots, K$, so that $N \equiv JK$. By rows, we mean beads of the same longitudinal position, θ .

We can define the principal moments of inertia I_1, I_2 , and I_3 by [Eqs. (16.7-17) and (16.7-18) of Ref. 4 or (13.6-17) and (13.6-18) of Ref. 5]

$$I_1 \equiv m \sum_{i=1}^N (R_{i2}^2 + R_{i3}^2), \quad (15)$$

$$I_2 \equiv m \sum_{i=1}^N (R_{i1}^2 + R_{i3}^2), \quad (16)$$

$$I_3 \equiv 2m \sum_{i=1}^N R_{i1}^2. \quad (17)$$

We design each Möbius macromolecule by rigidly connecting each bead to its nearest neighbors, center to center, with massless dimensionless rods.⁸ Adjacent rows are indexed identically,

$$I_1 \equiv m \sum_{j=1}^J \sum_{k=1}^K \left(\{R + s_k \cos \frac{1}{2} \tau \theta_j\}^2 \sin^2 \theta_j + s_k^2 \sin^2 \frac{1}{2} \tau \theta_j \right), \quad (18)$$

$$I_2 \equiv m \sum_{j=1}^J \sum_{k=1}^K \left(\{R + s_k \cos \frac{1}{2} \tau \theta_j\}^2 \cos^2 \theta_j + s_k^2 \sin^2 \frac{1}{2} \tau \theta_j \right), \quad (19)$$

$$I_3 \equiv 2m \sum_{j=1}^J \sum_{k=1}^K \{R + s_k \sin \frac{1}{2} \tau \theta_j\}^2 \cos^2 \theta_j. \quad (20)$$

By *indexed identically*, we mean that, for each row j , all beads have the same value of θ . From Eqs. (18) and (19), we learn that, if identically indexed beads are spaced evenly along and across the strip, $I_1 = I_2$. We call such Möbius macromolecules *axisymmetric*.

Hassager derives the expression for the shear relaxation function from general rigid bead-rod theory for axisymmetric macromolecules,^{17,18}

$$G(s) \equiv (2\eta_s + n\zeta L^2 a) \delta(s) + nkTbe^{-s/\lambda} \quad (21)$$

in which [Eqs. (16.7-38) of Ref. 4 or Eqs. (13.6-44), (13.6-45), and (13.6-46) of Ref. 5]

$$a \equiv \frac{2I_1 + I_3}{6mL^2} - \frac{(I_1 - I_3)^2}{5mL^2 I_1}, \quad (22)$$

$$b \equiv \frac{3(I_1 - I_3)^2}{5I_1^2}, \quad (23)$$

$$v \equiv \frac{6mL^2}{I_1}. \quad (24)$$

The three quantities in Eq. (21), a, b , and λ , thus define completely the differences in linear viscoelastic behaviors arising between different axisymmetric Möbius macromolecules. Whereas we associate

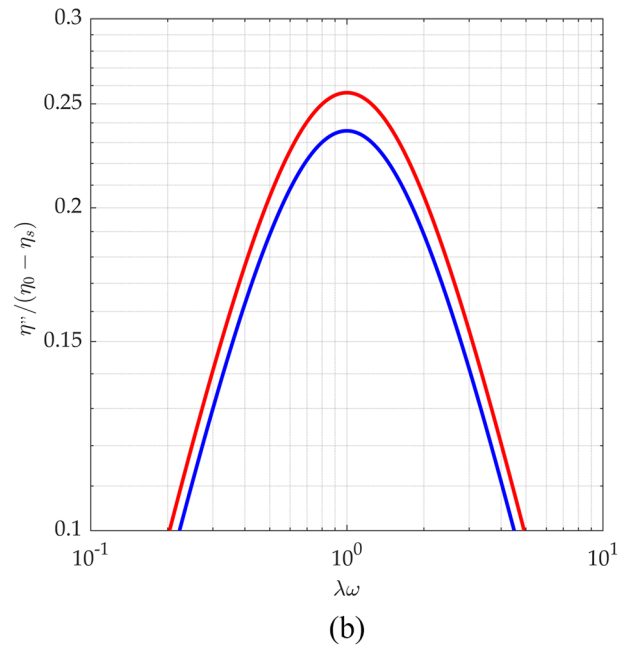
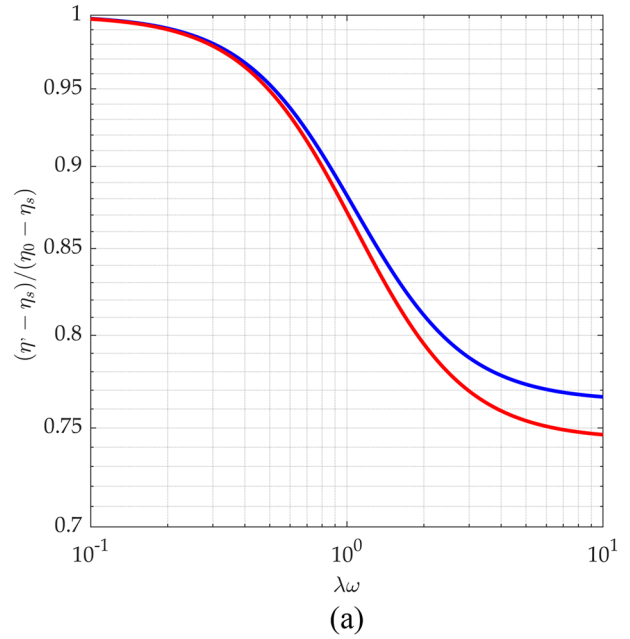


FIG. 3. [(a) and (b)] Effect of band width on the viscoelastic response [Eqs. (1) and (2)] of one twist Möbius bands. Three rows of beads with aspect ratio ten (blue) (Fig. 11) and seven rows of beads with aspect ratio ten (red).

a with the Dirac delta function contribution to the relaxation function given by Eq. (21), we associate b with the dying exponential. We call a , b , and v the *orientation constants* of the macromolecule.

The relaxation time can be expressed as

$$\lambda \equiv \frac{\zeta I_1}{6mkT} \equiv \frac{\zeta L^2}{vkT}, \tag{25}$$

where

$$\zeta \equiv 3\pi d\eta_s. \tag{26}$$

For later convenience, we define

$$\lambda_0 \equiv \frac{\zeta L^2}{12kT} = \frac{\pi d\eta_s L^2}{4kT}, \tag{27}$$

which we will use below.

From Ref. 17 (Chap. 16 of Refs. 4, 6, or 9), we learn that the value of $2b/av$ reflects *lopsidedness*, namely, the extent to which the macromolecule deviates from a spherically symmetric structure.

The minimum value of $2b/av$ is 0, obtained for spherically symmetric structures such as rigid regular octahedra (Macromolecule 5 of Ref. 9), and the maximum is $3/2$ for long slender bodies such as the rigid dumbbell (Macromolecule 1 in Table 4 of Ref. 9).

We classify macromolecules as prolate or oblate. By *prolate*, we mean that the macromolecule MIE is longer than it is wide. By *oblate*, we mean that the MIE is wider than it is long. Otherwise put, oblate and prolate macromolecules depart differently from spherical symmetry.

Dividing Eq. (25) by Eq. (27) normalizes the relaxation time of the general macromolecule to that of the simplest,

$$\frac{\lambda}{\lambda_0} \equiv \frac{12}{v}, \tag{28}$$

which we will use below.

Equations (22)–(24) imply the quadratic

$$a^2 v^2 + \frac{2}{3}(b-9)av + \frac{1}{9}(b^2 - 33b + 81) = 0 \tag{29}$$

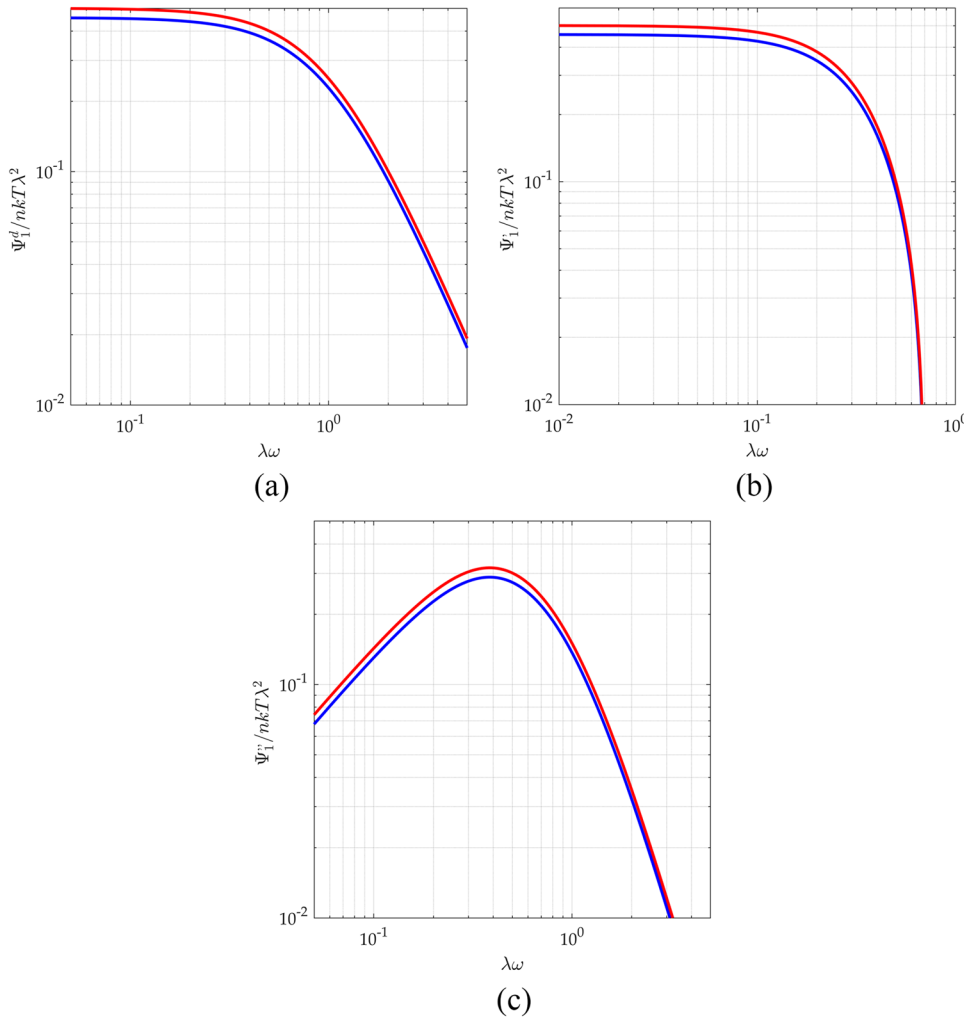


FIG. 4. [(a)–(c)] Effect of band width on the first normal stress difference [Eqs. (4)–(6)] of one twist Möbius bands. Three rows of beads with aspect ratio ten (**blue**) (Fig. 11) and seven rows of beads with aspect ratio ten (**red**).

whose prolate lower branch is given by

$$av = \frac{9 - b - \sqrt{15b}}{3} \tag{30}$$

and whose oblate upper branch is given by

$$av = \frac{9 - b + \sqrt{15b}}{3}. \tag{31}$$

From Eqs. (29)–(31), we learn that every axisymmetric macromolecule occupies one and only one position on either the upper or lower branch.

The simple shapes given by parametric equation (7) are not to be confused with the more complicated shapes arising when thick flat elastic strips are curved into cylindrical or twisted bands. These more complicated shapes are governed by solid mechanics.^{19–21}

III. RESULTS

Tables III–VI compare the moments of inertia, orientation constants, lambda ratios, and zero-shear properties for every Möbius macromolecule studied in this paper. Table III includes the results for Möbius bands of three rows with aspect ratio $R/w = 20$. By R/w , we mean the ratio of the radius of the circle of support, R , to the band width, w , of the Möbius macromolecule. Table IV includes the results for Möbius bands of three rows with an aspect ratio of ten. Table V includes the results for Möbius bands of three rows with an aspect ratio of ten. Table VI includes the results for Möbius bands of three rows with an aspect ratio of seven.

From Columns 9 and 10 of Table III–VI, we learn that the zero-shear viscosities and first normal stress coefficients, made dimensionless with λ , for the untwisted Möbius macromolecule are much higher than any of its twisted counterparts. By contrast, we also learn that the zero-shear viscosities and first normal stress coefficients, made dimensionless with λ , for the twisted Möbius macromolecules do not differ from one another. From Table VII, on the other hand, we learn that the zero-shear viscosities and first normal stress coefficients, made dimensionless with λ_0 , do differ significantly and without pattern.

A. Twists

Figure 1 shows the effect of the number of twists on the viscous and elastic response of Möbius band macromolecules. We find that for the dimensionless real part of the complex viscosity [Eq. (1)], the results fall on just three curves: one for zero twists [Eq. (9)], another lower one for an odd number [Eq. (7) with τ odd], and an even lower one for an even number [Eq. (7) with τ even]. This difference in $\eta'(\omega)$ increases with frequency [Fig. 1(a)]. We also find that for *minus* the dimensionless imaginary part of the complex viscosity [Eq. (2)], the results also fall on just three curves: one for zero twists, another higher one for an odd number, and an even higher one for an even number. This difference in $\eta''(\omega)$ does not vary with frequency [Fig. 1(b)]. We thus find that the effect of twisting the Möbius macromolecule on the parts of the complex viscosity is binary. This binary dependence on twist parity surprised us.

Figure 2 shows the effect of the number of twists on each of the three parts of the dimensionless complex first normal stress

coefficient response of Möbius band macromolecules. We find that for the dimensionless displacement value of the first normal stress coefficient [Eq. (4)], the results fall on just two curves: one for zero twists and the other higher one for twisted, be the number of twists

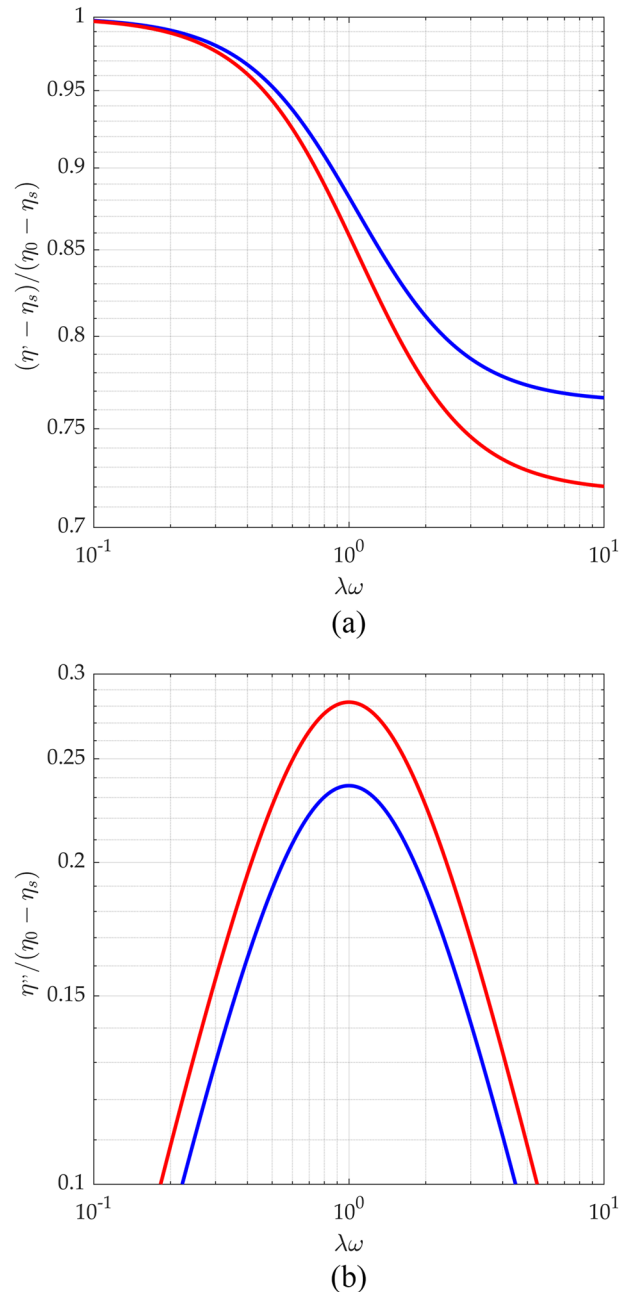


FIG. 5. [(a) and (b)] Effect of aspect ratio on the viscoelastic response [Eqs. (1) and (2)] of one twist Möbius macromolecules. Three rows of beads with aspect ratio ten (blue) (Fig. 11) and three rows of beads with aspect ratio twenty (red).

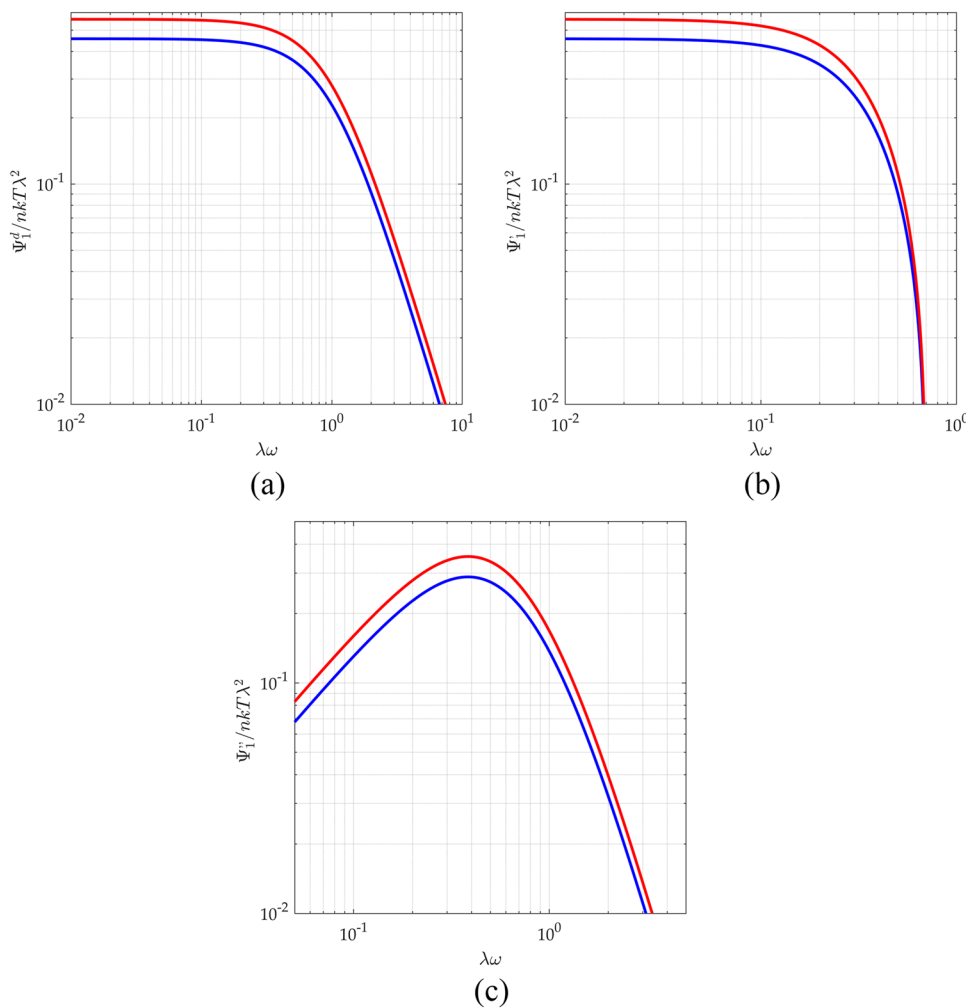


FIG. 6. [(a)–(c)] Effect of aspect ratio on the first normal stress difference [Eqs. (4)–(6)] of one twist Möbius bands. Three rows of beads with aspect ratio ten (blue) (Fig. 11) and three rows of beads with aspect ratio twenty (red).

even or odd. This difference decreases with frequency [Fig. 2(a)]. Similarly, we find that for the part in-phase with $\cos 2\omega t$ [Eq. (5)], the results also fall on just two curves, and their difference also decreases with frequency [Fig. 2(b)]. We find likewise for *minus* the part out-of-phase with $\cos 2\omega t$, Eq. (6) [Fig. 2(c)]. By contrast with the parts of the complex viscosity [Fig. 1], we find that the effect of twisting the Möbius macromolecule on the in-phase and out-of-phase parts of the first normal stress coefficient is not binary. Our findings of binary twist parity for η^* , and not for Ψ_1^d or Ψ_1^* , establish intuitive expectations for future work on twisted macromolecules.

B. Band width

To study the effect of band width, we compare a Möbius macromolecule with three rows of beads and an aspect ratio of ten to a Möbius macromolecule with seven rows of beads with the same aspect ratio of ten. *Band width* is the width of the Möbius macromolecule and is not to be confused with *band width* of signal processing.

Figure 3 shows the effect of Möbius macromolecule band width on the viscous and elastic response of Möbius band macromolecules.

We find that for the dimensionless real part of the complex viscosity [Eq. (1)], the increase in band width lowers the curve. This difference in $\eta'(\omega)$ increases with frequency [Fig. 3(a)]. We also find that for *minus* the dimensionless imaginary part of the complex viscosity

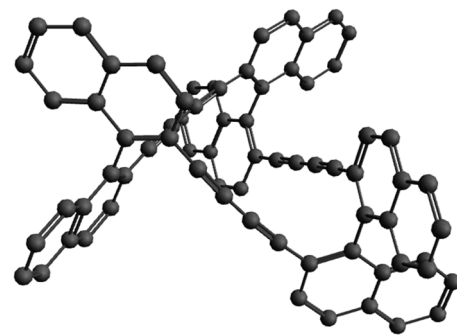


FIG. 7. The Möbius macromolecule triply twisted annulene.³

TABLE VIII. Möbius macromolecule triply twisted annulene.

Twists	I_1	I_3	a	b	ν	$2b/av$	λ/λ_0	$\frac{\eta_0 - \eta_s}{nk_B T \lambda}$	$\frac{\Psi_{1,0}}{nk_B T \lambda^2}$
3	705.6461	1051.8263	376.5535	0.1444	0.0085	0.0769	1411.2921	1.7453	0.3310

[Eq. (2)], the increase in band width increases the peak value. This difference in $\eta''(\omega)$ does not vary with frequency [Fig. 3(b)].

Figure 4 shows the effect of the band width on the first normal stress of Möbius band macromolecules. We find that for the dimensionless displacement value of the first normal stress coefficient [Eq. (4)], a decrease in band width lowers the curve. This difference decreases with frequency [Fig. 4(a)]. Similarly, we find that for the part in-phase with $\cos 2\omega t$ [Eq. (5)], a decrease also lowers the curve [Fig. 4(b)]. We find likewise for *minus* the part out-of-phase with $\cos 2\omega t$, Eq. (6) [Fig. 4(c)].

C. Aspect ratio

To study the effect of aspect ratio, we compare a Möbius macromolecule with three rows of beads and an aspect ratio of ten to a Möbius macromolecule with seven rows of beads with the same aspect ratio of ten.

Figure 5 shows the effect of the chain aspect ratio on the viscous and elastic response of Möbius band macromolecules. We find that for the dimensionless real part of the complex viscosity [Eq. (1)], the increase in aspect ratio lowers the curve. This difference in $\eta'(\omega)$ increases with frequency [Fig. 5(a)]. We also find that for *minus* the dimensionless imaginary part of the complex viscosity [Eq. (2)], the increase in aspect ratio increases the peak value. This difference in $\eta''(\omega)$ does not vary with frequency [Fig. 5(b)].

Figure 6 shows the effect of the aspect ratio on the first normal stress of Möbius band macromolecules. We find that for the dimensionless displacement value of the first normal stress coefficient [Eq. (4)], decreasing the aspect ratio lowers the curve. This difference decreases with frequency [Fig. 6(a)]. Similarly, we find that for the part in-phase with $\cos 2\omega t$ [Eq. (5)], a decrease also lowers the curve [Fig. 6(b)]. We find likewise for *minus* the part out-of-phase with $\cos 2\omega t$, Eq. (6) [Fig. 6(c)].

IV. WORKED EXAMPLE: TRIPLY TWISTED MÖBIUS ANNULENE

We next turn our attention to a specific organic Möbius macromolecule, the triply twisted annulene, shown in Fig. 7, whose bead centers are given in the supplementary material of Ref. 3. Proceeding from these bead centers and following the method of Sec. II, we generate Table VIII from general rigid bead-rod theory. Then, using Eqs. (1) and (2) with Table VIII, we predict the parts of the complex viscosity for a suspension of triply twisted annulene in small-amplitude oscillatory shear flow, after which we plot these in Fig. 8. To our knowledge and presumably due to the scarcity of the compound, the complex viscosity of such a suspension has yet to be measured. Using Eqs. (4)–(6) with Table VIII, we predict all three parts of the first normal stress coefficient response for a suspension

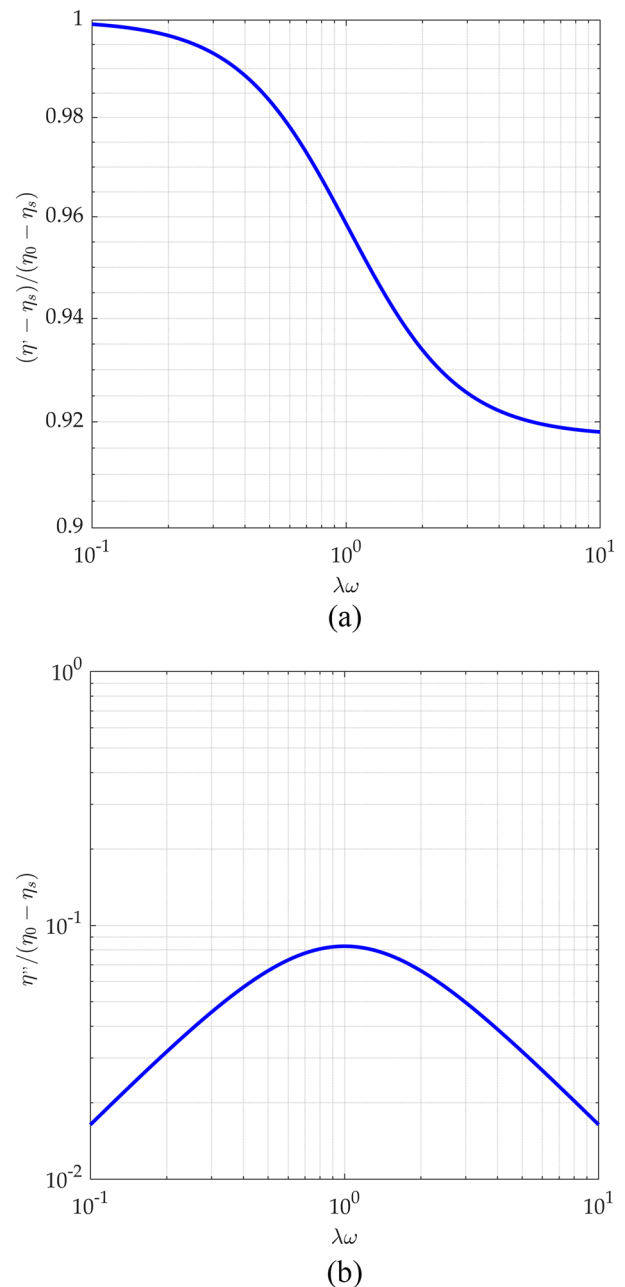


FIG. 8. General rigid bead rod theory for twisted annulene (Fig. 1 of Ref. 3, Fig. 7). Complex viscosity: (a) in-phase with $\dot{\gamma}$ [Eq. (1)] and (b) *minus* out-of-phase with $\dot{\gamma}$ [Eq. (2)].

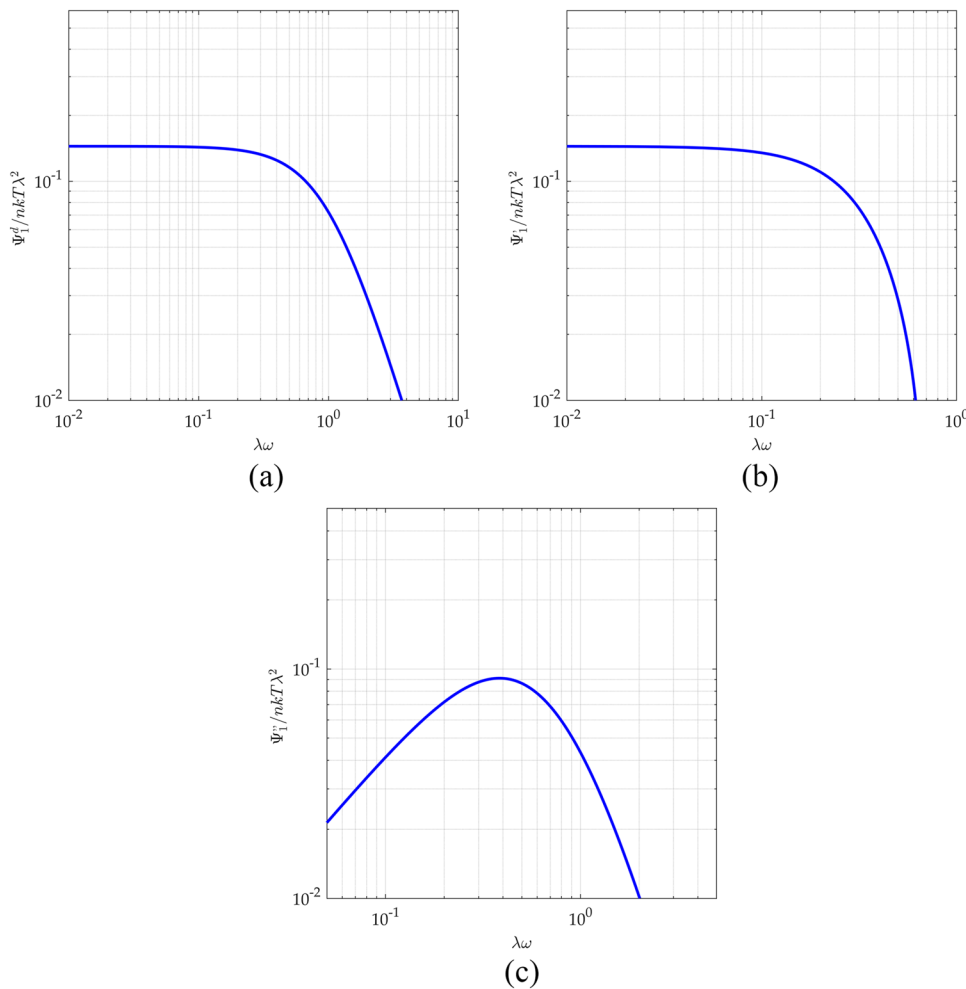


FIG. 9. General rigid bead rod theory for twisted annulene (Fig. 1 of Ref. 3, Fig. 7). First normal stress coefficient: (a) displacement value [Eq. (4)] and (b) in-phase with $\cos 2\omega t$ [Eq. (5)]. (c) *Minus* out-of-phase with $\cos 2\omega t$ [Eq. (6)].

of triply twisted annulene in small-amplitude oscillatory shear flow and plot these in Fig. 9. As far as we know, the first normal stress coefficient of such a suspension has yet to be measured.

From Table VIII, we learn that a triply twisted annulene $\nu \cong 0.0085$, which when inserted into Eq. (3) yields

$$\lambda\dot{\gamma}^0 \ll 83.19, \tag{32}$$

which defines small-amplitude for triply twisted annulene in oscillatory shear flow.

V. CONCLUSION

In this paper, we calculate the complex viscosity [Eqs. (1) and (2)] and the corresponding first normal stress coefficient [Eqs. (4)–(6)] in small-amplitude [Eq. (3)] oscillatory shear flow of suspensions of Möbius macromolecules from general rigid bead–rod theory. Figures 10 and 11 provide a representation of Möbius macromolecules with differing amounts of twists, from various angles. We discover binary behaviors for both the real and imaginary parts of

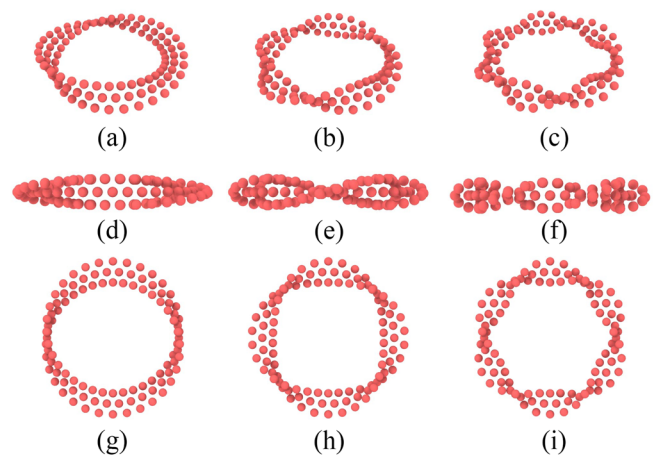


FIG. 10. [(a)–(i)] Even twisted Möbius bands.

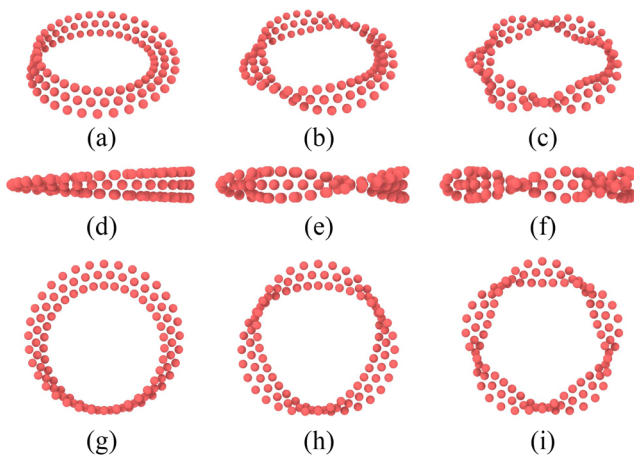


FIG. 11. [(a)–(i)] Odd twisted Möbius bands.

the complex viscosity [Figs. 1(a) and 1(b), respectively]. By *binary*, we mean that the result depends only on the Möbius macromolecule twist parity. By contrast, we discover that the behaviors for all three parts of the first normal stress coefficients in small-amplitude oscillatory shear flow [Figs. 2(a)–2(c)] are not binary.

We study macromolecules whose bead positions all lie on the surfaces of Möbius bands, described by Eq. (7), which includes the cylinder as a special case [Eq. (9)]. Equation (7) thus describes Möbius bands constructed by cutting and twisting a right circular cylinder. By contrast, Möbius bands can also be constructed by cutting and twisting a frustrated disk, and these surfaces are given by

$$\begin{bmatrix} x \\ y \\ z \end{bmatrix} = \begin{bmatrix} \{R + s \sin \frac{1}{2} \tau \theta\} \cos \theta \\ \{R + s \sin \frac{1}{2} \tau \theta\} \sin \theta \\ s \cos \frac{1}{2} \tau \theta \end{bmatrix}, \quad 0 \leq \theta \leq 2\pi, \quad (33)$$

$$-\frac{1}{2}w \leq s \leq \frac{1}{2}w, \tau = 0, 1, 2, \dots,$$

where all bands described by this intersect at the *circle of support* of radius, R [Eq. (8)]. Without twists, $\tau = 0$, and Eq. (33) reduces to

$$\begin{bmatrix} x \\ y \\ z \end{bmatrix} = \begin{bmatrix} \{R + s\} \cos \theta \\ \{R + s\} \sin \theta \\ 0 \end{bmatrix}, \quad 0 \leq \theta \leq 2\pi, -\frac{1}{2}w \leq s \leq \frac{1}{2}w, \quad (34)$$

which represents the *frustrated disk*.

Generalizing Eqs. (7) and (33) yields for the surfaces of all Möbius bands constructed by cutting and twisting either cylinders ($\kappa = 0$) or frustrated disks ($\kappa = \pi/2$)

$$\begin{bmatrix} x \\ y \\ z \end{bmatrix} = \begin{bmatrix} \{R + s \sin(\kappa + \frac{1}{2} \tau \theta)\} \cos \theta \\ \{R + s \sin(\kappa + \frac{1}{2} \tau \theta)\} \sin \theta \\ s \cos(\kappa + \frac{1}{2} \tau \theta) \end{bmatrix}, \quad 0 \leq \theta \leq 2\pi, 0 \leq \kappa \leq \frac{\pi}{2}, \quad (35)$$

$$-\frac{1}{2}w \leq s \leq \frac{1}{2}w, \tau = 0, 1, 2, \dots$$

We leave the study of this broader class of Möbius macromolecules for another day.

Since Möbius bands can evert,²² in principle, so might Möbius macromolecules during flow, including oscillatory shear flow, the flow at issue in this paper. However, our general rigid bead–rod theory precludes eversion during flow. This being said, when everted, the principal moments of inertia of a Möbius macromolecule do not change. Our theory could be used to calculate the torque about the neutral axis of the Möbius macromolecules during flow. We could then see if this torque ever exceeds the critical torque for eversion. We leave this exploration for another day.

We have neglected interferences of solvent velocity profiles between adjacent beads. Called *hydrodynamic interactions*,²³ we leave this improvement for another day. Of course, general rigid bead–rod theory explains the elasticity of the liquid by means of macromolecular orientation alone. We also leave the role played by macromolecular compliance²⁴ in the rheology of Möbius macromolecules for another day.

In previous work, we managed to derive exact analytical expressions for the properties in Tables III–VIII of simpler architectures including shish-kebabs, rigid rings, and planar star-shaped polymers (see Table XV of Ref. 9). We have proceeded numerically from the bead positions. For the simplest general rigid bead–rod theory representation of Möbius macromolecules, one might proceed analytically from Eq. (14). Following the method of Sec. II, one might also attack interlocking Möbius macromolecules of like or unlike twist parities. We leave these interesting tasks for another day.

For rigid dumbbells, we know of reasonable predictions for the steady shear viscosity and first normal stress difference material functions of polymeric liquids (see Sec. 6 of Ref. 14). The rigid-dumbbell suspension has also been shown to predict accurately the Cox–Merz rule.²⁵ Of course, we can bridge general rigid bead–rod theory with continuum mechanics to arrive at approximate relations for the steady shear material functions. We would do so by inserting the bridging relations Eqs. (64)–(66) of Ref. 9 into the steady shear material functions for Oldroyd 8-constant fluids [Eqs. (74)–(76) of Ref. 9]. The result could then be tested against the measured structure dependencies of the steady shear material functions. We leave this task for another day. When using the references cited herein, it is best to be mindful of corresponding ganged errata in Ref. 26.

ACKNOWLEDGMENTS

We thank Mona Kanso of Queen’s University for her helpful correspondence. A.J.G. is indebted to the Faculty of Applied Science and Engineering of Queen’s University at Kingston for its support through a Research Initiation Grant (RIG). This research was undertaken, in part, thanks to support from the Canada Research Chairs program of the Government of Canada for the Natural Sciences and Engineering Research Council of Canada (NSERC) Tier 1 Canada Research Chair in Rheology. The work of E.F. and N.M. was supported by the Okinawa Institute of Science and Technology Graduate University with subsidy funding from the Cabinet Office, Government of Japan.

DATA AVAILABILITY

The data that support the findings of this study are available within the article.

REFERENCES

- ¹J. H. Piette, A. J. Giacomin, and M. A. Kalso, "Complex viscosity of helical and doubly helical polymeric liquids from general rigid bead-rod theory," *Phys. Fluids* **31**(11), 111904 (2019).
- ²R. Herges, "Topology in chemistry: Designing Möbius molecules," *Chem. Rev.* **106**, 4820–4842 (2006).
- ³G. R. Schaller, F. Topić, K. Rissanen, Y. Okamoto, J. Shen, and R. Herges, "Design and synthesis of the first triply twisted Möbius annulene," *Nat. Chem.* **6**(7), 608–613 (2014).
- ⁴R. B. Bird, O. Hassager, R. C. Armstrong, and C. F. Curtiss, *Dynamics of Polymeric Liquids*, 1st ed. (John Wiley & Sons, New York, 1977), Vol. 2.
- ⁵R. B. Bird, R. C. Armstrong, and O. Hassager, *Dynamics of Polymeric Liquids*, 2nd ed. (Wiley, New York, 1977), Vol. 2.
- ⁶M. A. Kalso, "Polymeric liquid behavior in oscillatory shear flow," M.S. thesis, Polymers Research Group, Chemical Engineering Department, Queen's University, Kingston, Canada, July 23, 2019.
- ⁷M. A. Kalso, A. J. Giacomin, C. Saengow, and J. H. Piette, "Diblock copolymer architecture and complex viscosity," *Int. J. Mod. Phys. B* **34**, 2040110 (2020).
- ⁸R. B. Bird, A. J. Giacomin, A. M. Schmalzer, and C. Aumnate, "Dilute rigid dumbbell suspensions in large-amplitude oscillatory shear flow: Shear stress response," *J. Chem. Phys.* **140**, 074904 (2014).
- ⁹M. A. Kalso, A. J. Giacomin, C. Saengow, and J. H. Piette, "Macromolecular architecture and complex viscosity," *Phys. Fluids* **31**, 087107 (2019).
- ¹⁰C. Saengow, A. J. Giacomin, and C. Kolutawong, "Exact analytical solution for large-amplitude oscillatory shear flow from Oldroyd 8-constant framework: Shear stress," *Phys. Fluids* **29**(4), 043101 (2017).
- ¹¹C. Saengow and A. J. Giacomin, "Normal stress differences from Oldroyd 8-constant framework: Exact analytical solution for large-amplitude oscillatory shear flow," *Phys. Fluids* **29**(12), 121601 (2017).
- ¹²C. Saengow, A. J. Giacomin, and A. S. Dimitrov, "Unidirectional large-amplitude oscillatory shear flow of human blood," *Phys. Fluids* **31**(11), 111903 (2019).
- ¹³M. A. Kalso and A. J. Giacomin, "Polymer branching and first normal stress differences in small-amplitude oscillatory shear flow," *Can. J. Chem. Eng.* **98**(7), 1444–1455 (2020).
- ¹⁴R. B. Bird, H. R. Warner, and D. C. Evans, "Kinetic theory and rheology of dumbbell suspensions with Brownian motion," *Adv. Polym. Sci.* **8**, 1–90 (1971).
- ¹⁵J. H. Piette, L. M. Jbara, C. Saengow, and A. J. Giacomin, "Exact coefficients for rigid dumbbell suspensions for steady shear flow material function expansions," *Phys. Fluids* **31**(2), 021212 (2019).
- ¹⁶Kalso Van Gulp.
- ¹⁷M. A. Kalso and A. J. Giacomin, "Van Gulp-Palmen relations for long-chain branching from general rigid bead-rod theory," *Phys. Fluids* **32**(3), 033101 (2020).
- ¹⁸O. Hassager, "On the kinetic theory and rheology of multibead models for macromolecules," Ph.D. thesis, Chemical Engineering, University of Wisconsin, Madison, WI, 1973.
- ¹⁹R. Fosdick and E. Fried, *The Mechanics of Ribbons and Möbius Bands* (Springer, The Netherlands, 2016).
- ²⁰D. M. Kleiman, D. F. Hinz, Y. Takato, and E. Fried, "Influence of material stretchability on the equilibrium shape of a Möbius band," *Soft Matter* **12**(16), 3750–3759 (2016).
- ²¹E. Couturier, "Folded isometric deformations and banana-shaped seedpod," *Proc. R. Soc. A* **472**, 20150760 (2016).
- ²²J. Schönke and E. Fried, "Single degree of freedom everting ring linkages with nonorientable topology," *Proc. Natl. Acad. Sci. U. S. A.* **116**(1), 90–95 (2019).
- ²³J. H. Piette, C. Saengow, and A. J. Giacomin, "Hydrodynamic interaction for rigid dumbbell suspensions in steady shear flow," *Phys. Fluids* **31**(5), 053103 (2019).
- ²⁴J. H. Piette, C. Saengow, and A. J. Giacomin, "Zero-shear viscosity of Fraenkel dumbbell suspensions," *Phys. Fluids* **32**(6), 063103 (2020).
- ²⁵W. E. Stewart and J. P. Sørensen, "Hydrodynamic interaction effects in rigid dumbbell suspensions. II. Computations for steady shear flow," *Trans. Soc. Rheol.* **16**(1), 1–13 (1972).
- ²⁶J. H. Piette, N. Moreno, E. Fried, and A. J. Giacomin, "The complex viscosity of Möbius macromolecules," PRG Report No. 070, QU-CHEE-PRGTR-2020-70, Polymers Research Group, Chemical Engineering Department, Queen's University, Kingston, Canada, 2020, pp. 0–35.